

Collective excitations in supercritical fluids: Analytical and molecular dynamics study of “positive” and “negative” dispersion

Taras Bryk,^{1,2,a)} Ihor Mryglod,^{1,2} Tullio Scopigno,^{3,4} Giancarlo Ruocco,^{3,4} Federico Gorelli,^{4,5} and Mario Santoro^{4,5}

¹*Institute for Condensed Matter Physics, National Academy of Sciences of Ukraine, UA-79011 Lviv, Ukraine*

²*Institute of Applied Mathematics and Fundamental Sciences, Lviv National Polytechnic University, UA-79013 Lviv, Ukraine*

³*Dipartimento di Fisica, Università di Roma “La Sapienza”, I-00185, Roma, Italy*

⁴*IPCF-CNR, Università di Roma, I-00185, Roma, Italy*

⁵*European Laboratory for Non Linear Spectroscopy, Sesto Fiorentino, Firenze, Italy*

(Received 10 December 2009; accepted 10 May 2010; published online 8 July 2010)

The approach of generalized collective modes is applied to the study of dispersion curves of collective excitations along isothermal lines of supercritical pure Lennard-Jones fluid. An effect of structural relaxation and other nonhydrodynamic relaxation processes on the dispersion law is discussed. A simple analytical expression for the dispersion law in the long-wavelength region of acoustic excitations is obtained within a three-variable viscoelastic model of generalized hydrodynamics. It is shown that the deviation from the linear dependence in the long-wavelength region can be either “positive” or “negative” depending on the ratio between the high-frequency (elastic) and isothermal speed of sound. An effect of thermal fluctuations on positive and negative dispersion is estimated from the analytical solution of a five-variable thermoviscoelastic model that generalizes the results of the viscoelastic treatment. Numerical results are reported for a Lennard-Jones supercritical fluid along two isothermal lines $T^*=1.71, 4.78$ with different densities and discussed along the theoretical expressions derived. © 2010 American Institute of Physics. [doi:10.1063/1.3442412]

I. INTRODUCTION

The theoretical treatment of collective dynamics in liquids is an extremely complicated problem because of the existence of different time scales of microscopic processes. Only on macroscopic spatial and time scales the analytical expressions for time correlation functions $F_{ij}(k, t)$ and spectrum of hydrodynamic collective modes can be obtained. The leading contributions to experimentally measured quantities (such as the dynamic structure factor $S(k, \omega)$, where k and ω are wave number and frequency, respectively) are well established only in hydrodynamic limit when $k \rightarrow 0$, $\omega \rightarrow 0$.¹⁻³ For the case of simple monoatomic liquids, three hydrodynamic equations reflect in fact the local conservation laws and describe only the dynamical processes on large spatial and time scales comparing with the average interatomic distance and characteristic molecular times, i.e., when liquids are treated as continuum without any detail of the atomic structure. Beyond the hydrodynamic region, where most of real experiments using X-ray or neutron scattering techniques and computer molecular dynamics (MD) simulations are located, the short-time processes with finite lifetime and a spatial nanoscale become very important and essentially contribute to the shape of dynamic structure factors. Therefore, a lot of efforts have been made in order to derive analytical expressions for the hydrodynamic time correlation functions [in particular, for the density-density time correlation function $F_{nn}(k, t)$,

which are simply connected via inverse time-Fourier transform to $S(k, \omega)$] generalizing the known hydrodynamic results and that could be used beyond the hydrodynamic region. One of the successful attempts, a *nonlocal* mode coupling theory (MCT),^{4,5} can potentially explain dynamical phenomena in a very broad range of temperatures and densities, however due to the necessity of evaluating intermediate integrations over wave numbers it can be used practically in a limited number of applications. Hence less sophisticated schemes of generalized hydrodynamics based on the memory function formalism (MFF) in the local form¹ are often more useful for practical needs.

According to hydrodynamics the only long-wavelength propagating processes in liquids are the longitudinal sound excitations with linear dispersion law $\omega(k)=c_s k$ and a damping which is quadratic in wave numbers $\sigma(k)=\Gamma k^2$, where c_s and Γ are the adiabatic speed of sound and damping coefficient, respectively. For single-component liquids the hydrodynamics yields only two nonpropagating relaxation processes. One of them, which couples to longitudinal propagating modes, corresponds to thermal relaxation and is defined by thermal diffusivity. Another relaxation process is not coupled to longitudinal processes in isotropic liquids and is connected with shear viscosity.¹⁻³ Upon increasing wave numbers, i.e., when wavelengths reduce and approach the molecular length scale, the dispersion law of acoustic excitations changes essentially from that of the hydrodynamic regime. Usually for dense liquids the deviation at small wave numbers corresponds to bending up the dispersion curve and

^{a)}Electronic mail: bryk@icmp.lviv.ua.

is called “positive” dispersion,^{6,7} although recently “negative” dispersion cases in supercritical fluids have been reported.⁸ To date two mechanisms are recognized to be mainly responsible for the “positive dispersion” in pure liquids: nonlocal coupling effects between hydrodynamic modes described within the MCT (Ref. 4) and local coupling between acoustic excitations and nonhydrodynamic structural relaxation obtained within the MFF.⁹ However, there were no systematic theoretical and experimental studies of the density or pressure dependence of positive or negative deviation from hydrodynamic dispersion law, except the inelastic neutron scattering experiments and subsequent calculations, based on MCT for liquid Ar at 120 K.¹⁰ The microscopic mechanism responsible for positive dispersion in MCT (Ref. 4) is the nonlocal (with different wave numbers) coupling of hydrodynamic relaxation and propagating modes. The MCT yields the following expression for the dispersion law of acoustic excitations:

$$\omega(k) = c_s k + \alpha_s k^{5/2} + O(k^{11/4}) + \dots, \quad (1)$$

where the coefficient α_s can be estimated from a sophisticated expression given in Ref. 10, which requires the knowledge of explicit density dependences of adiabatic speed of sound $c_s(n)$ and thermal expansion coefficient $\alpha_T(n)$. The analytical expression for the dispersion law (1) is an asymptotic expansion and is valid only in a small wave number region, usually very close to the boundary of hydrodynamic regime. The third term in expansion (1) contains $k^{11/4}$ and to date nobody was able to calculate it in order to estimate its sign and relative contribution with respect to the second term. Even calculations of the prefactor α_s and its density dependence are very scarce in the literature. The results on α_s , reported in Ref. 10 gave evidence that for dense liquids such as Ar at 120 K, the prefactor α_s is positive, and contains a strong contribution from thermal processes and reduces with increasing density. This means that the behavior of the dispersion following from the first two terms in Eq. (1) should be expected as a reduction of the positive dispersion of acoustic excitations in dense liquids by increasing density or pressure. However, recent IXS experiments on supercritical Ar (Refs. 11 and 12) resulted in a completely different tendency for the pressure dependence of positive sound dispersion in the supercritical region. It was observed that the positive dispersion reduces with decreasing density and practically vanishes at some density.

Besides, recently there appeared a report on a change of dispersion curves in liquid nitrogen for seven thermodynamic points at constant pressure.¹³ A transformation from adiabatic to isothermal speed of sound was observed in the sound dispersion of fluid nitrogen close to supercritical conditions. Such a change in the dispersion curve of collective excitations was treated as a consequence of the absence of a structural relaxation process, known to be responsible for the positive deviation from the linear dispersion law beyond the hydrodynamic regime. Recently there appeared also a theoretical study within the MCT, which was focused on structural relaxation processes in liquids and glasses¹⁴ and one of the results was a possible negative deviation from the linear dispersion law for long-wavelength acoustic excitations.

Over the last 15 years, another theoretical method of analysis of collective dynamics in liquids has proved its ability to correctly describe the dispersion of acoustic collective excitations and wave number dependence of nonpropagating relaxation processes. The approach of generalized collective modes (GCM) represents collective dynamic processes in liquids as a sum of contributions from hydrodynamic and nonhydrodynamic (kinetic) collective modes.^{15,16} This approach is based on the eigenvalue solutions of the generalized Langevin equation with coupling effects between different processes taken in local approximation (with the same wave numbers) in contrast to MCT. The microscopic mechanism for changes in hydrodynamic dispersion law of collective excitations in GCM is due to coupling of acoustic excitations with nonhydrodynamic processes such as structural relaxation, nonhydrodynamic heat relaxation, or propagating heat waves. This approach is much simpler with respect to the MCT one, and gives the possibility of tracing down the role of different nonhydrodynamic processes by analytically treating simplified dynamical models, which yielded very transparent and useful analytical results in different regions of (k, ω) -plane. The analytical GCM results were obtained for describing the following nonhydrodynamic processes in liquids: structural relaxation,¹⁷ kinetic heat relaxation,¹⁸ optically excitations in binary liquids,^{19,20} heat waves,²¹ and charge waves in molten salts.²²

The aim of this study is to perform a numerical and analytical GCM analysis of dispersion of collective excitations along several isothermal lines on the phase diagram of Lennard-Jones fluids. The obtained analytical expressions within a local-coupling GCM theory could point out what kind of microscopic processes are responsible for positive or negative sound dispersion at the boundary of hydrodynamic regime.

The remaining paper is organized as follows: in the next section we report a GCM analysis of collective dynamics in supercritical Lennard-Jones fluids along two isothermal lines on the phase diagram; in section III two dynamic models (viscoelastic and thermoviscoelastic ones for pure liquids) are solved analytically in the long-wavelength limit in order to study the origin of deviation from linear dispersion law of acoustic excitations on the boundary of hydrodynamic region; and in the last section we give the conclusions of this study.

II. COLLECTIVE DYNAMICS IN SUPERCRITICAL LENNARD-JONES FLUIDS: NUMERICAL GCM ANALYSIS

In this section we will discuss the dispersion law of collective excitations in fluids obtained within the five-variable dynamical model.¹⁸ Analytical solutions in terms of five eigenmodes are possible only in the limit $k \rightarrow 0$. Beyond the hydrodynamic region, for an arbitrary k , only numerical GCM analysis of the five-variable model can yield the k -dependence of all eigenmodes.

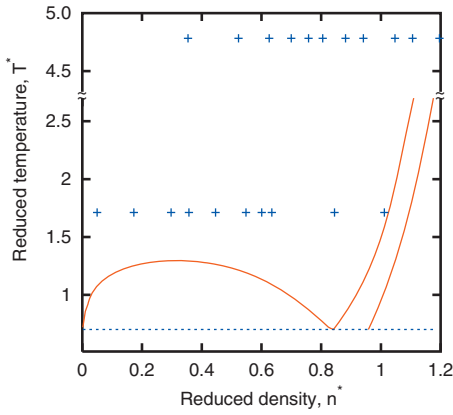


FIG. 1. Thermodynamic points on phase diagram along the isothermal lines $T^*=1.71$ and $T^*=4.78$ chosen for this study. The standard reduction of units was used: $n^*=n\sigma_{LJ}^3$ and $T^*=T/\varepsilon_{LJ}$.

A. Method of calculations and details of MD simulations

MD simulations were performed in microcanonical ensemble for a model system of 2000 particles interacting via Lennard-Jones potentials with cutoff radius of 12 Å. Production runs of 300 000 time steps were performed along the two isothermal lines at reduced temperatures $T^*=1.71$ and $T^*=4.78$, shown on phase diagram of Lennard-Jones fluid in Fig. 1. The Lennard-Jones parameters $\sigma_{LJ}=3.405$ Å and $\varepsilon_{LJ}=119.8$ K were used in actual simulations, and the standard reduction of units was applied: $n^*=n\sigma_{LJ}^3$, $T^*=T/\varepsilon_{LJ}$. Since we made use of the standard Lennard-Jones parameters of argon we have to mention that in this theoretical study, we are aimed to explain by a combination of computer simulations and analytical theory an effect, which is general for all pure fluids. In case of a particular application of this theory to the analysis of scattering experiments on supercritical Ar more precise *ab initio* potentials^{23,24} can be used, especially in the case of Ar fluid at high pressures and temperatures.

The time step in MD simulations was 2 fs. For every sixth configuration the following five dynamic variables: particle density $n(k,t)$, density of longitudinal momentum $J^L(k,t)$, heat density $h(k,t)$, and first time derivatives of $J^L(k,t)$ and $h(k,t)$, were sampled, saved and used later in subsequent calculations of relevant static and time correlation functions needed for the estimation of generalized thermodynamic quantities and matrix elements within the GCM approach. Here

$$n(k,t) = \frac{1}{\sqrt{N}} \sum_{j=1}^N e^{-ikr_j},$$

$$J^L(k,t) = \frac{m}{\sqrt{N}} \sum_{j=1}^N \frac{\mathbf{k} \cdot \mathbf{v}_j}{k} e^{-ikr_j}, \quad (2)$$

$$h(k,t) = \varepsilon(k,t) - \frac{\langle \varepsilon_k n_{-k} \rangle}{\langle n_k n_{-k} \rangle} n(k,t),$$

where

$$\varepsilon(k,t) = \frac{1}{\sqrt{N}} \sum_{j=1}^N \varepsilon_j e^{-ikr_j},$$

with $\varepsilon_j(t)$, $\mathbf{v}_j(t)$, and $\mathbf{r}_j(t)$ being total single-particle energy, velocity, and position of j th particle at time moment t , respectively, and N , m are the number and mass of particles. The averages $\langle \varepsilon_k n_{-k} \rangle$ and $\langle n_k n_{-k} \rangle$ correspond to the standard instantaneous energy-density and density-density correlators. We stress that the direct sampling of heat density and its first time derivative is necessary for the correct analysis of collective dynamics beyond the hydrodynamic region. Most theoretical and simulations studies of collective dynamics in liquids completely ignore effects connected with heat fluctuations, or treat them on the level of fitting procedures.

The main equations of the GCM approach for the case of pure systems can be found in Ref. 16. The general scheme of GCM analysis consists in the calculation of the generalized hydrodynamic matrix $\mathbf{T}(k)$ on a chosen basis set of dynamic variables and finding its eigenvalues and eigenvectors. The pairs of complex-conjugated eigenvalues correspond to propagating modes, while purely real eigenvalues have the meaning of inverse lifetimes of corresponding nonpropagating relaxation processes. The corresponding eigenvectors allow to calculate so-called mode strengths (weights) of the dynamic eigenmodes in relevant time correlation functions or the dynamic structure factors. In this study the matrix elements of the generalized hydrodynamic matrix $\mathbf{T}(k)$ were estimated for each k -point directly from MD simulations avoiding any fitting procedure. The GCM analysis of MD-derived time correlation functions was performed within the thermoviscoelastic five-variable dynamic model for the case of longitudinal dynamics

$$\mathbf{A}^{(5)}(k,t) = \{n(k,t), J^L(k,t), h(k,t), \dot{J}^L(k,t), \dot{h}(k,t)\}. \quad (3)$$

For the analysis of collective dynamics the density dependence of adiabatic speed of sound c_s is needed. This quantity is a characteristic of sound propagation in hydrodynamic regime. Another quantity, the high-frequency speed of sound c_∞ , reflects the elastic mechanism of sound propagation. The adiabatic speed of sound

$$c_s = \left[\frac{\gamma k_B T}{m S(k=0)} \right]^{1/2},$$

was calculated for each thermodynamic point from the long-wavelength limit of a ratio $\sqrt{\gamma(k)/S(k)}$, which is a smooth function of wave number and can be easily extrapolated to a value at $k=0$. The high-frequency speed of sound was estimated from the long-wavelength asymptote of wave number-dependent quantity

$$c_\infty(k) = \frac{1}{k} \left[\frac{\langle J^L(-k) J^L(k) \rangle}{\langle J^L(-k) J^L(k) \rangle} \right]^{1/2}.$$

In Figs. 2 and 3, one can see the calculated density dependence of adiabatic and high-frequency speed of sound for the two isothermal lines shown in the phase diagram of Fig. 1.

Another important thermodynamic quantity, which reflects the strength of coupling between thermal and viscous processes in liquids, is the ratio of specific heats at constant

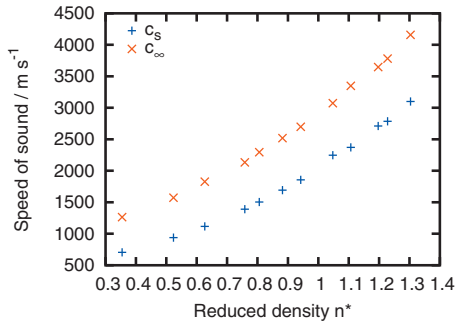


FIG. 2. Calculated adiabatic and high-frequency speed of sound along the isothermal line $T^*=4.38$.

pressure and constant volume γ . For $\gamma=1$ the density and thermal fluctuations are decoupled. The values of γ calculated along two chosen isothermal lines are shown in Fig. . In the high-density region, the ratio of specific heats is close to unity like in case of liquid metals. By reducing the density, γ increases and, at the temperature $T^*=1.71$, shows a pronounced peak close to reduced density $n^*=0.3$. According to the NIST database²⁵ for supercritical argon close to the density $n^*=0.3$ the ratio of specific heats as a function of density reaches maximum, which in the case of $T^*=1.71$ is much sharper than for the high-temperature state. This gives evidence that by approaching to the critical point from the high-temperature side a strong coupling between density and thermal fluctuations takes place.

B. Spectra of collective excitations

The GCM theoretical results for some restricted set of dynamic variables have sense only in the case when the GCM analytical expressions can reproduce MD-derived dynamic structure factors $S(k, \omega)$. For the case of the five-variable dynamic model $A^{(5)}(k, t)$ the quality of GCM replicas is provided by first five frequency moments of $S(k, \omega)$, which coincide for MD- and GCM-derived dynamic structure factors, as well as additional sum rules connected in GCM theory with equivalence of density-density, density-energy and energy-energy correlation times in theory and simulations. All this permits to obtain very nice reproduction of dynamic structure factors on the boundary of hydrodynamic regime by the GCM theory (see Fig. 5). Different intensities of central and side peaks of $S(k, \omega)$ in the hydrodynamic regime are defined by the Landau–Placzek ratio,¹

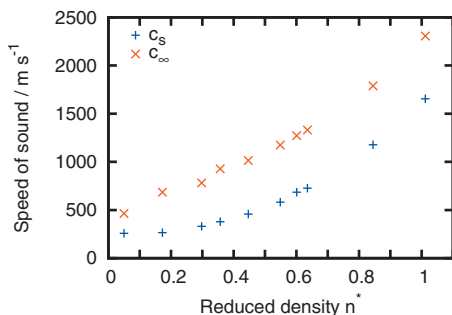


FIG. 3. Calculated adiabatic and high-frequency speed of sound along the isothermal line $T^*=1.71$.

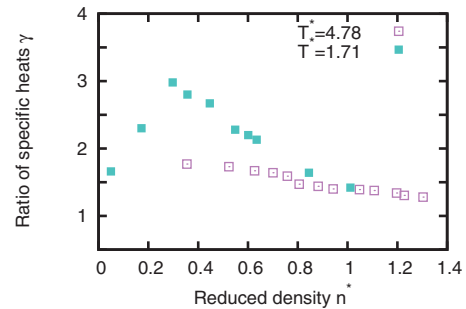


FIG. 4. Calculated dependence of the ratio of specific heats γ on density along the studied isothermal lines on phase diagram.

and in our case, Fig. 5 shows that the GCM theory can nicely reproduce collective effects in supercritical Ar in quite wide region of the ratio of specific heats γ , which is a measure of coupling between thermal and viscous processes.

The imaginary parts $\omega(k)$ of complex-conjugated pairs of GCM eigenvalues of the generalized hydrodynamic matrix $\mathbf{T}(k)$,

$$z_{\pm}(k) = \sigma(k) \pm i\omega(k),$$

correspond to the dispersion of collective excitations. The calculated dispersion curves for several densities are shown in Figs. 6 and 7. By dashed lines, the linear dispersion law with corresponding values of adiabatic speed of sound c_s is shown. The values of c_s for different n were estimated independently from the calculations of $z_{\pm}(k)$ as described above.

In Figs. 6 and 7, the general tendencies in the dispersion change with density are: (i) the reduction of the slope of the linear dispersion law at small exchanged momentum with decreasing density, which is in agreement with Figs. 2 and 3; (ii) the reduction of the rotonlike minimum with decreasing

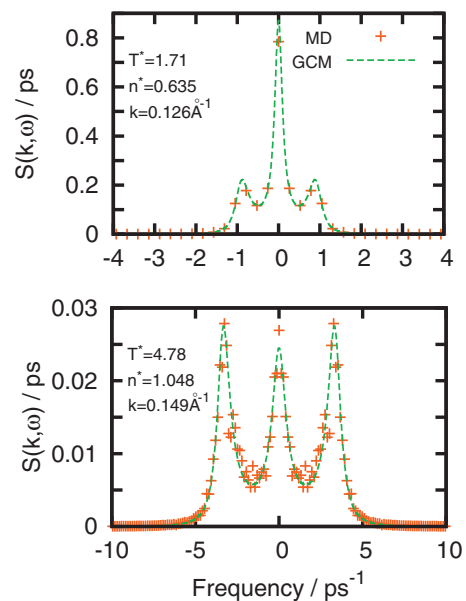


FIG. 5. Reproduction of dynamic structure factors calculated directly from MD data (plus symbols) by the GCM 5-variable dynamic model (solid line) for low $T^*=1.71$ (top frame) and high $T^*=4.78$ (bottom frame) temperatures. Relative intensities of central to side peaks are defined by $(\gamma-1)$ via Landau–Placzek ratio that is essentially different for the two thermodynamic points shown.

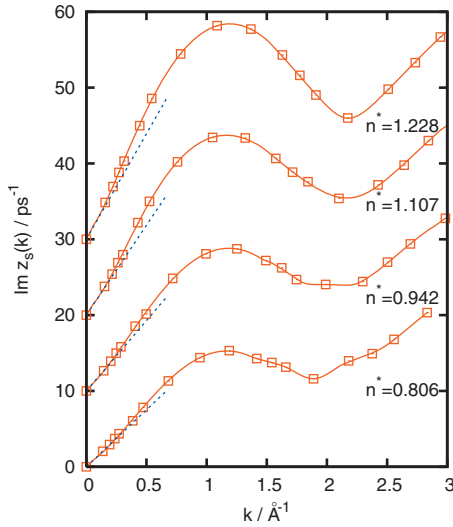


FIG. 6. Dispersion of collective excitations for different densities at $T^* = 4.78$. Dashed line shows the linear hydrodynamic dispersion law with hydrodynamic speed of sound c_s .

density, (iii) the reduction of the bending up of the dispersion curve in the long-wavelength region, i.e., the reduction of positive dispersion, with decreasing density; and (iv) increasing of the width of region, where apparent speed of sound almost coincides with c_s , with decreasing density.

Interesting that for some low-density states the eigenvalues can even correspond to a negative dispersion of collective excitations, as it is shown by the bottom curve in the long-wavelength region of Fig. 7. However, with increasing wave numbers the dispersion of collective excitations at $n^* = 0.357$ does not keep reducing its slope, but for $k \sim 0.7 \text{ \AA}^{-1}$ the dispersion curve starts again to bend up implying that perhaps different processes have an effect on sound dispersion curve in different regions of wave numbers.

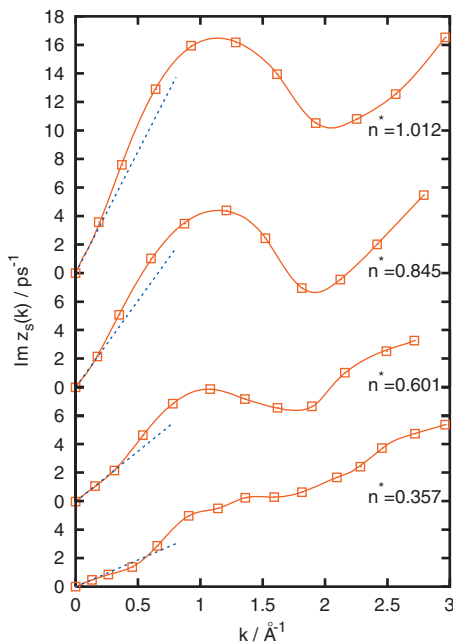


FIG. 7. Dispersion of collective excitations for different densities at $T^* = 1.71$. Dashed line shows the linear hydrodynamic dispersion law with hydrodynamic speed of sound c_s .

In order to explain the positive and negative dispersions observed in our GCM calculations we aimed to obtain the analytical expressions for eigenvalues $z_{\pm}(k)$ within the same dynamic model.

III. SOUND DISPERSION AT THE BOUNDARY OF HYDRODYNAMIC REGIME: ANALYTICAL GCM EXPRESSIONS

Let us first consider a simplified viscoelastic model in order to obtain a compact expression for the positive dispersion, while the subsequent treatment performed within the five-variable thermoviscoelastic model will generalize the obtained expression to the case of coupled density and thermal fluctuations.

A. Decoupled density and heat fluctuations

A simple dynamical model, which consists of three dynamical variables

$$\mathbf{A}^{(3)}(k, t) = \{n(k, t), J^L(k, t), \dot{J}^L(k, t)\}, \quad (4)$$

is well known as the viscoelastic one, because in addition to the hydrodynamic variables of particle density and mass-current density, a nonhydrodynamic variable connected with the elastic properties of the liquid is taken into account. Since the extended variable $\dot{\mathbf{J}}(k, t)$ is connected to the stress tensor $\sigma_{\alpha\beta}(k, t)$ via²⁶

$$\frac{d}{dt} \mathbf{J}(k, t) = i\mathbf{k} \hat{\sigma}(k, t),$$

there appear in the viscoelastic approach the quantities from the theory of elasticity.

For this basis set $\mathbf{A}^{(3)}(k, t)$, when one does not take the heat fluctuations into account, the correlation time can be obtained from the hydrodynamic one $\tau_{nn}^{(hyd)}(k)$ defined as

$$\tau_{nn}(k) = \frac{1}{S(k)} \int_0^{\infty} F_{nn}(k, t) dt,$$

by setting $\gamma=1$ in the analytical hydrodynamic expression for $F_{nn}(k, t)$ (Ref. 27)

$$\tau_{nn}(k) = \frac{D_L}{c_s^2 + 4D_L^2 k^2}.$$

Now the generalized hydrodynamic matrix generated on the basis set (4) can be written down as follows:

$$\mathbf{T}^{(ve)}(k) = \begin{pmatrix} 0 & -i\frac{k}{m} & 0 \\ 0 & 0 & -1 \\ -imkc_T^2 \frac{c_{\infty}^2 - c_T^2}{D_L} & k^2 c_{\infty}^2 & \frac{c_{\infty}^2 - c_T^2}{D_L} \end{pmatrix}, \quad (5)$$

where the following shortcut was introduced $k^2 c_{\infty}^2 = \langle J^L J^L \rangle / \langle J^L J^L \rangle$ with c_{∞} being the high-frequency (elastic) speed of sound. The quantities D_L and c_T in Eq. (5) are the kinematic viscosity and isothermal speed of sound. One can easily find eigenvalues of the matrix $\mathbf{T}^{(ve)}(k)$ within the precision of $O(k^2)$, which are a pair propagating modes

$$z_{\pm}(k) = \frac{D_L}{2}k^2 \pm ic_T k \equiv \sigma(k) \pm i\omega(k), \quad (6)$$

and a kinetic collective mode

$$d_{ve}(k) = \frac{c_{\infty}^2 - c_T^2}{D_L} - D_L k^2 \equiv d^0 - D_L k^2, \quad (7)$$

which tends to a nonzero constant d^0 in the long-wavelength limit. The factor $(c_{\infty}^2 - c_T^2)$ is usually called as the “strength” of the structural relaxation process. Besides, the constant d^0 goes to zero when the kinematic viscosity tends to infinity that means an almost infinite relaxation time of the mode $d_{ve}(k)$ at the glass transition. All this implies that the kinetic mode $d_{ve}(k)$ is connected to the structural α -relaxation.

The expression for the sound dispersion (imaginary part of eigenvalues $z_{\pm}(k)$) does not show any effect due to coupling of acoustic excitations to the relaxation kinetic mode of structural relaxation $d_{ve}(k)$, which can appear only in the $O(k^3)$ order in the sound dispersion. In order to estimate the imaginary part of the complex eigenvalues corresponding sound dispersion within the precision of $O(k^3)$, one can derive from Eq. (5) an effective equation for sound eigenmodes by eliminating the known real eigenvalue $d_{ve}(k)$ [see Eq. (7)]. The effective equation reads

$$z^2 - D_L k^2 z + \frac{c_T^2 d^0}{d_{ve}(k)} k^2 = 0, \quad (8)$$

and now the sound dispersion can be obtained as

$$\begin{aligned} \omega_{ve}(k) &= c_T k \sqrt{1 + \frac{D_L}{d^0} k^2 - \frac{D_L^2}{4c_T^2} k^2 + O(k^4)} \\ &= c_T k + \beta_{ve} k^3 + \dots \end{aligned} \quad (9)$$

In the expression under the square root there are two contributions proportional to k^2 : the first one is positive and comes from the coupling of acoustic excitations with structural relaxation, and the second contribution, the negative one, is the standard renormalization down of the dispersion law due to the damping effects. One can obtain the first correction to the linear viscoelastic dispersion law, proportional to the k^3 having the following coefficient:

$$\beta_{ve} \approx c_T \frac{D_L^2}{8} \frac{5 - (c_{\infty}/c_T)^2}{c_{\infty}^2 - c_T^2}. \quad (10)$$

The most interesting consequence is that, in general, the sign of the $O(k^3)$ correction to the linear dispersion law can be different depending on the ratio between the high-frequency speed of sound and the isothermal one. Note, that the high-frequency speed of sound is always higher than the adiabatic one c_s (as it is shown in Figs. 2 and 3) that in its turn is $\sqrt{\gamma}$ times higher than c_T . The analysis of MD simulations leads to the fact that a negative dispersion can be observed for the low-density states, and this finding supports MD results shown in Fig. 7.

B. Thermoviscoelastic model for pure fluids

Now our task is to take into account the coupling of density fluctuations to thermal processes and find out how

this effect contributes to the deviation of the dispersion curve from the linear hydrodynamic dispersion law. We want to obtain the analytical expressions for the eigenmodes in a pure fluid, within a five-variable thermoviscoelastic model in the long-wavelength limit.¹⁸ The dynamical model $\mathbf{A}^{(5)}(k, t)$ [Eq. (3)] contains additionally to the viscoelastic model the heat density $h(k, t)$ and the corresponding extended variable $\dot{h}(k, t)$. The five eigenmodes within the precision of $O(k^2)$ for the thermoviscoelastic model are reported in Ref. 18 and contained three hydrodynamic modes

$$d_1(k) = D_T k^2, \quad (11)$$

$$z_{\pm}(k) = \Gamma k^2 \pm i[c_s k + O(k^3)],$$

exactly as they appear in the hydrodynamic approach, and two kinetic relaxing modes

$$d_2(k) = d_2^0 - D_L k^2 + (\gamma - 1)\Delta k^2, \quad (12)$$

and

$$d_3(k) = d_3^0 - \gamma D_T k^2 - (\gamma - 1)\Delta k^2, \quad (13)$$

where the following shortcuts were introduced:

$$d_2^0 = \frac{c_{\infty}^2 - c_s^2}{D_L},$$

and

$$d_3^0 = \frac{c_V}{m\lambda} \left[G^h - \frac{(\gamma - 1)}{\kappa_T} \right],$$

and

$$\Delta = \frac{d_2^0 d_3^0}{d_3^0 - d_2^0} \frac{D_T}{D_L c_s^2} (D_T - D_L)^2.$$

The quantities D_T , Γ , G^h , and κ_T correspond to thermal diffusivity, sound damping coefficient, heat rigidity modulus and isothermal compressibility, respectively. The last terms in right hand sides of Eqs. (12) and (13) appear only due to coupling between the heat and density fluctuations. When this coupling is neglected, i.e., $\gamma=1$, one obtains for the kinetic modes $d_2(k)$ and $d_3(k)$ the same expressions as within the separated treatment of two-variable heat- and three-variable viscoelastic dynamical models [at $\gamma=1$ the kinetic mode $d_2(k)$ is reduced to Eq. (7)].

Let us try now to look at the complex eigenvalues of the thermoviscoelastic dynamic model within the precision of $O(k^3)$. After straightforward calculations one yields

$$z_s(k) = \Gamma k^2 \pm i(c_s k + \beta k^3), \quad (14)$$

where the coefficient at k^3 reads as follows:

$$\beta = -\frac{\Gamma^2}{2c_s} - (\gamma - 1)D_T \frac{D_L - D_T}{2c_s} + \frac{c_s D_L}{2d_2^0} + (\gamma - 1) \frac{c_s(\gamma - 1)D_T}{2d_3^0}. \quad (15)$$

It can be observed that in comparison with the results of the three-variable viscoelastic dynamic model β contains two additional contributions: Negative and positive ones. The first and third terms in Eq. (15) have an analogy in the vis-

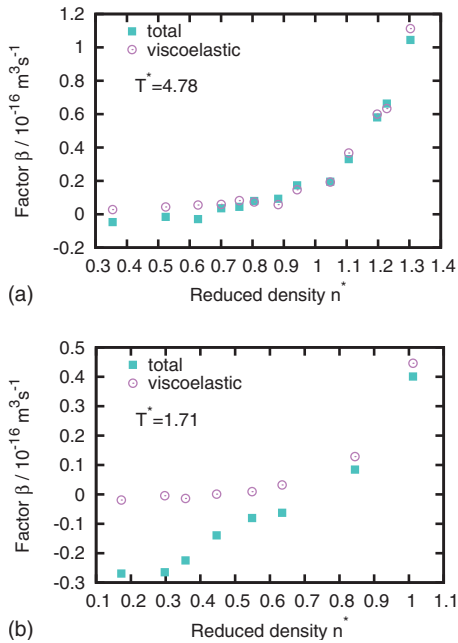


FIG. 8. Dependence of factor β [Eq. (16)] on density for two temperatures $T^* = 4.78$ and $T^* = 1.71$ (closed boxes). Open circles correspond to viscoelastic contribution to the β .

coelastic model and correspond to contributions from damping and coupling with the structural relaxation process, respectively. Combining the terms with prefactor $(\gamma - 1)$ one yields the following expression:

$$\beta = \frac{c_s D_L^2}{8} \frac{5 - (c_\infty/c_s)^2}{c_\infty^2 - c_s^2} - (\gamma - 1) D_T \left[\frac{6D_L + (\gamma - 5)D_T}{8c_s} - \frac{c_s}{2d_3^0} \right]. \quad (16)$$

In the case when $\gamma \approx 1$ the estimate for the sound dispersion at the boundary of hydrodynamic regime within the thermo-viscoelastic model reads

$$\omega(k) \approx c_s k + \frac{c_s D_L^2}{8} \frac{5 - (c_\infty/c_s)^2}{c_\infty^2 - c_s^2} k^3, \quad (17)$$

which is identical to Eq. (10) for the case of $\gamma = 1$, with c_s being equal to c_T . In Fig. 8, the results of numerical calculations of the factor β from Eq. (16) for two temperatures using the GCM data as input are presented. The strength of contribution from the first term in Eq. (16) is shown by open circles. The evident difference between the total β and viscoelastic contribution is attributed to thermal processes [second term in Eq. (16)]. One can see that for the high-temperature state $T^* = 4.78$ the positive dispersion is completely defined by the viscoelastic mechanism, i.e., due to coupling of collective excitations with structural relaxation. Most interesting is the fact that positive dispersion practically vanishes for that temperature around $n^* \approx 0.8$. For smaller temperatures ($T^* = 1.71$) being closer to the critical point the effect of thermal contribution is much stronger due perhaps to the strong increase of γ as is shown in Fig. 4. Our calculations give evidence that at low-temperatures for densities $n^* > 0.75$ the dispersion curve in the long-wavelength region shows a positive dispersion, while for $n^* < 0.6$ the

dispersion can be negative in a narrow region of wave numbers close to hydrodynamic regime. A comparison of the results of our analytical study for factor β (Fig. 8) that defines the deviation from linear dispersion law in long-wavelength region, with the GCM dispersion curves of collective excitations shown in Figs. 6 and 7 gives evidence that the proposed analytical approach can reasonably reflect the behavior of positive and negative dispersion versus density, and most important it points out the microscopic processes responsible for the observed effects.

One has to keep in mind that the obtained analytical expressions correspond to asymptotic expansions in long-wavelength region. They correctly reflect the change in positive dispersion and emergence of negative dispersion as observed from the GCM-MD numerical calculations. Hence, it would be very useful to estimate the width of wave number region, where these expressions would be valid. The issue of the density dependence of the positive dispersion is strictly connected with understanding of how the range of hydrodynamic regime changes with density. From the wave number dependence of hydrodynamic relaxation mode $d_1(k)$, see Eq. (11), and nonhydrodynamic relaxation processes $d_2(k)$, $d_3(k)$, Eqs. (12) and (13), one can expect that strong deviation from the hydrodynamic behavior $\sim k^2$ will be observed for the case when the lifetimes of hydrodynamic and nonhydrodynamic processes become comparable. This can be treated as the boundary of hydrodynamic regime, and the collective modes that corresponded to hydrodynamic processes do not have anymore hydrodynamic $\sim k^2$ dependence of real parts of the eigenvalues. Approximately, the upper bound of the hydrodynamic region (or the width of hydrodynamic regime) can be defined as the point, where the lowest kinetic relaxation mode $d_2(k)$, which corresponds to the structural relaxation, becomes equal to the hydrodynamic relaxation mode, connected with thermal diffusivity $d_1(k) = D_T k^2$. From such a condition one obtains straightforwardly a value of corresponding wave number

$$k_{hd} \approx \left[\frac{(c_\infty^2 - c_s^2)}{D_L(D_L + D_T - (\gamma - 1)\Delta)} \right]^{1/2}. \quad (18)$$

One can see that the width of the hydrodynamic regime is mainly controlled by the kinematic viscosity. When the viscosity diverges like at the glass transition, the hydrodynamic region vanishes, i.e., the region of wave numbers (even on macroscopic spatial scales) where one can observe viscous properties, sound propagation with the adiabatic speed of sound and other hydrodynamic asymptotes specific for the liquid state disappears.

In connection with our study of positive and negative dispersion, the Eq. (18) estimates the range of validity of expressions for factor β . Namely, within this region of wave numbers the effect of nonhydrodynamic relaxation processes on dispersion of collective modes is clearly seen, because in the limit $k \rightarrow 0$ the effect of nonhydrodynamic processes is absent, and for $k > k_{hd}$ it is already completely taken into account. As we have mentioned above, for $k > k_{hd}$ the calculated dispersion curve can show another bending up, even after initial “negative dispersion,” which implies another process making an effect on sound propagation on specific

spatial scales. Our theoretical approach took into account the effects of structural α -relaxation, while another nonhydrodynamic process of μ -relaxation^{28,29} was not explicitly taken in the theoretical treatment in long-wavelength limit. It is possible that the μ -process, connected with topological disorder^{28,29} makes an effect on sound dispersion curves, being responsible for observed maxima on $\omega_s(k)$ in the region $k > k_{hd}$. Another possibility for additional bending-up of the sound dispersion for wave numbers $k > k_{hd}$ is the coupling to heat waves,²¹ which do not exist in long-wavelength region and emerge in the fluids usually in the region of wave numbers $\sim 0.5\text{--}0.8 \text{ \AA}^{-1}$.

IV. CONCLUSIONS

We performed a numerical and analytical GCM study of dispersion of collective excitations in pure fluids aiming to explain the origin and density dependence of positive dispersion of long-wavelength acoustic modes. The GCM approach is based on extended basis sets of dynamic variables, which permits to take explicitly into account local coupling effects between hydrodynamic and nonhydrodynamic processes. In this study we solved analytically in the long-wavelength region a three-variable viscoelastic model, which permits to take into account coupling of longitudinal collective modes with nonhydrodynamic process of structural relaxation in complete neglect of thermal processes. More sophisticated dynamic model, a five-variable thermoviscoelastic one, generalizes results of the three-variable treatment on the case with thermal fluctuations are turned on. Main results of our study can be formulated as follows:

- (i) Positive dispersion reduces with decrease of density (and pressure), in contrast to prediction of MCT within the precision of $O(k^{5/2})$.¹⁰ Our simulations and analytical results are in complete agreement with recent IXS experiments on supercritical Ar (Ref. 12).
- (ii) Analytical expression (15) for the correction to hydrodynamic dispersion law derived for the case when thermal fluctuations are neglected gives evidence that structural relaxation can be responsible for both positive and negative dispersion depending on the ratio of high-frequency to adiabatic speeds of sound;
- (iii) Thermal contribution to the correction to linear hydrodynamic dispersion law is negative and can be very strong for densities close to critical point because of large value of ratio of specific heats γ . The GCM approach predicts possible observation of the negative dispersion for long-wavelength collective excitations in the region of densities close to the critical point.

ACKNOWLEDGMENTS

T.B. was supported by the Joint SFBRU-RFBR Program under Project No. $\Phi 28.2/037$. F.A.G. and M.S. have been supported by the European Community under Contract No. RII3-CT2003-506350. T.S. acknowledges support from the European Research Council under the European Community Seventh Framework Program FP7/2007-2013/ERC IDEAS Grant No. 207916.

- ¹J.-P. Boon and S. Yip, *Molecular Hydrodynamics* (McGraw-Hill, New York, 1980).
- ²N. H. March and M. P. Tosi, *Atomic Dynamics in Liquids* (Macmillan, London, 1976).
- ³J.-P. Hansen and I. R. McDonald, *Theory of Simple Liquids* (Academic, London, 1986).
- ⁴M. H. Ernst and J. R. Dorfman, *J. Stat. Phys.* **12**, 311 (1975).
- ⁵J. Bosse, W. Götze, and M. Lücke, *Phys. Rev. A* **18**, 1176 (1978).
- ⁶U. Balucani and M. Zoppi, *Dynamics of the liquid state* (Clarendon, Oxford, 1994).
- ⁷T. Scopigno, G. Ruocco, and F. Sette, *Rev. Mod. Phys.* **77**, 881 (2005).
- ⁸F. Bencivenga, A. Cunsolo, M. Krisch, G. Monaco, G. Ruocco, and F. Sette, *Europhys. Lett.* **75**, 70 (2006).
- ⁹T. Scopigno, U. Balucani, G. Ruocco, and F. Sette, *J. Phys.: Condens. Matter* **12**, 8009 (2000).
- ¹⁰I. M. de Schepper, P. Verkerk, A. A. van Well, and L. A. de Graaf, *Phys. Lett. A* **104**, 29 (1984).
- ¹¹F. A. Gorelli, M. Santoro, T. Scopigno, M. Krish, T. Bryk, G. Ruocco, and R. Ballerini, *Appl. Phys. Lett.* **94**, 074102 (2009).
- ¹²G. Simeoni, Ph.D. thesis, Università La Sapienza, Rome, 2009; G. Simeoni, T. Bryk, F.A. Gorelli, M. Krisch, G. Ruocco, M. Santoro, T. Scopigno, *Nat. Phys.* **6**, 503 (2010).
- ¹³F. Bencivenga, A. Cunsolo, M. Krisch, G. Monaco, G. Ruocco, and F. Sette, *J. Chem. Phys.* **130**, 064501 (2009).
- ¹⁴S.-H. Chong, *Phys. Rev. E* **74**, 031205 (2006).
- ¹⁵I. M. de Schepper, E. G. D. Cohen, C. Bruin, J. C. van Rijs, W. Montfrooij, and L. A. de Graaf, *Phys. Rev. A* **38**, 271 (1988).
- ¹⁶I. M. Mryglod, I. P. Omelyan, and M. V. Tokarchuk, *Mol. Phys.* **84**, 235 (1995).
- ¹⁷T. Bryk and I. Mryglod, *Condens. Matter Phys.* **11**, 139 (2008).
- ¹⁸T. Bryk and I. Mryglod, *Condens. Matter Phys.* **7**, 471 (2004).
- ¹⁹T. Bryk and I. Mryglod, *J. Phys.: Condens. Matter* **12**, 6063 (2000).
- ²⁰T. Bryk and I. Mryglod, *J. Phys.: Condens. Matter* **14**, L445 (2002).
- ²¹T. Bryk and I. Mryglod, *Phys. Rev. E* **63**, 051202 (2001).
- ²²T. Bryk and I. Mryglod, *J. Phys.: Condens. Matter* **16**, L463 (2004).
- ²³D. E. Woon, *Chem. Phys. Lett.* **204**, 29 (1993).
- ²⁴J.-M. Bomont, J.-L. Bretonnet, T. Pfeleiderer, and H. Bertagnolli, *J. Chem. Phys.* **113**, 6815 (2000).
- ²⁵E. W. Lemmon, M. O. McLinden, and D. G. Friend, *Thermophysical Properties of Fluid Systems in NIST Chemistry WebBook, NIST Standard Reference Database Number 69*, edited by P. J. Linstrom and W. G. Mallard (National Institute of Standards and Technology, Gaithersburg MD, 2005), <http://webbook.nist.gov>.
- ²⁶A. Z. Akcasu and E. Daniels, *Phys. Rev. A* **2**, 962 (1970).
- ²⁷C. Cohen, J. W. H. Sutherland, and J. M. Deutch, *Phys. Chem. Liq.* **2**, 213 (1971).
- ²⁸T. Scopigno, G. Ruocco, F. Sette, and G. Viliani, *Phys. Rev. E* **66**, 031205 (2002).
- ²⁹T. Scopigno, L.-B. Suck, R. Angelini, F. Albergamo, and G. Ruocco, *Phys. Rev. Lett.* **96**, 135501 (2006).